



The self-trapping transition of one-magnon excitations coupled to acoustic phonons

D. Morais^a, M.L. Lyra^a, F.A.B.F. de Moura^a, W.S. Dias^{a,*}

^a Instituto de Física, Universidade Federal de Alagoas, Maceió, AL 57072-970, Brazil

ARTICLE INFO

Keywords:
Magnon
Phonon
Self-trapping
Nonlinearity

MSC:
82D40
93C10

ABSTRACT

We study the dynamics of one-magnon states coupled to the underlying harmonic oscillations of a linear lattice. We consider that small amplitude oscillations affect linearly the exchange couplings. Within an adiabatic approximation, the magnon dynamics is governed by an effective modified nonlinear Schrödinger equation. We provide a detailed numerical study of the magnon self-trapping transition. We accurately determine the critical nonlinearity χ_c above which a finite fraction of an initially localized spin excitation remains trapped. To this end, we analyze relevant quantities such as the return probability, participation number and Shannon entropy. We also follow the soliton dynamics showing that its velocity vanishes as $v \propto (\chi_c - \chi)^{1/2}$. The return probability is shown to be discontinuous at χ_c while the participation number displays a kink singularity.

1. Introduction

The dynamics of spin waves in complex magnetic systems under influence of interactions with magnetic fields or lattice vibrations has been a key condensed matter topic within the last decades [1–3]. According to the recent literature, the presence of elasticity as well as interaction between magnons and phonons were shown to be relevant within the context of distinct magnetic compounds [4–10]. Several works have shown experimentally that the presence of vibrational modes affects substantially the dynamics of spin excitations [4–7]. The presence of spin-phonon coupling, as well as its effects on the magnetic properties, was also reported to take place in some semiconductors [8,9]. In Ref. [10], the authors investigated films of the ferrimagnetic insulator Yttrium-Iron garnet under a non-uniform magnetic field. They demonstrated the conversion of coherent magnons generated by a microwave field into phonons that carries a net spin.

In which concerns the theoretical description of several magnetic systems, the Heisenberg Hamiltonian [11,12] has a successful trajectory [13–19]. In general, the exchange spin-spin coupling that is considered within the Heisenberg formalism can depend on the spin's positions as well as on their relative displacement. The role played by the magnon-phonon coupling has been explored in several systems [20–22]. The Heisenberg Hamiltonian was used, for example, to describe the conversion between magnons and phonons [23]. Moreover, it was also used to explain experimental data related to the phonon dynamics in magnetic systems [24] and the effect of spin-phonon coupling on the

colossal magneto-resistance of magnetic compounds [25].

In this work, we will study the dynamics of spin-waves in an anisotropic one-dimensional ferromagnetic system of spins $S = 1/2$. We will take in account the influence of vibrational modes on the spin-waves propagation, i.e., the coupling between one-magnon and acoustic phonon excitations. Within an adiabatic approximation, and considering that lattice vibrations can be treated according to the classical mechanics formalism, the magnon dynamics is governed by a modified discrete nonlinear Schrödinger equation (MDNLSE). In this sense, it depicts some similarities with the polaron phenomenon for electronic systems [26–32]. We will solve numerically the dynamic equation and follow the time evolution of an initially localized spin deviation. Some relevant quantities such as the return probability, participation number and Shannon entropy will be used to characterize the dynamic regimes. In particular, we will show that a finite fraction of the magnon-excitation remains trapped around its initial location above a critical nonlinear strength χ_c . For weaker nonlinearities, the magnon-excitation develops soliton-like fronts that propagate with a constant velocity v . The soliton velocity will be shown to vanish as a power-law when from below. The singular behavior of the return probability and participation number will be also unveiled.

2. Magnon-Phonon Hamiltonian and the effective MNLSE

We will consider a Heisenberg Hamiltonian in the anisotropic form $XXZ (H_{mag})$ to describe the spin-spin interactions along a linear lattice.

* Corresponding author.

E-mail address: wandearley@fis.ufal.br (W.S. Dias).

<https://doi.org/10.1016/j.jmmm.2020.166798>

Received 2 October 2019; Received in revised form 18 February 2020; Accepted 21 March 2020

Available online 23 March 2020

0304-8853/ © 2020 Elsevier B.V. All rights reserved.

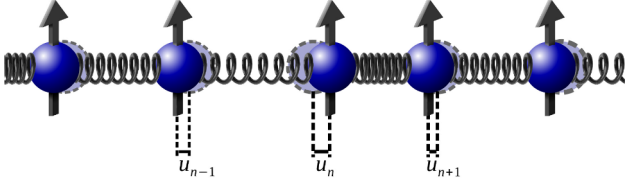


Fig. 1. Schematic representation of a spin linear lattice with effective harmonic springs coupling nearest-neighbor spins. The exchange interaction along the field direction is considered to be affected by the relative displacement of the pair of nearest-neighbor spins.

Classical harmonic oscillations will be considered to account for the lattice dynamics described by a Hamiltonian H_{latt} . The complete effective Hamiltonian is given by $H = H_{mag} + H_{latt}$. In Fig. 1 we show a schematic representation of the present model system. Each spin is coupled with its nearest neighbors by harmonic springs. u_n represents the position of spin n . The classical Hamiltonian describing the lattice dynamics is given by:

$$H_{latt} = \sum_{n=1}^N \left[\frac{M}{2} \dot{u}_n^2 + \frac{\kappa}{2} (u_{n+1} - u_n)^2 \right]. \quad (1)$$

M and κ represent the ion's mass and the spring constant respectively. We will consider that the $\omega \hbar \ll k_B T$ where $\omega = \sqrt{\kappa/M}$, k_B is the Boltzmann constant and T is the temperature. In this regime, the lattice dynamics can be treated within the classical mechanics formalism. We will consider the action of an external magnetic field H to promote a saturated ferromagnetic ground state. The magnetic field will be assumed to be large enough so that thermal fluctuations mainly produce states with single spin flips. In what follows, we will be interested in investigating how the dynamics of these one-magnon states are affected by the underlying lattice oscillations. In the sub-space of single spin-flip excitations, the Heisenberg Hamiltonian can be written as:

$$H_{mag} = E_0 + 2g\mu_B HS + \sum_{n=1}^N \{ 2S\hbar(J_{n,n+1}^Z + J_{n,n-1}^Z)c_n^\dagger c_n - 2S\hbar J_{n,n+1}^{XY}c_{n+1}^\dagger c_n - 2S\hbar J_{n,n-1}^{XY}c_{n-1}^\dagger c_n \}, \quad (2)$$

where $S = 1/2$ and $J_{n,m}^{Z(XY)}$ represent the exchange couplings between spins n and m along the Z direction and XY plane. The ground-state energy is given by $E_0 = -S^2 \sum_m J_{m,m\pm 1}^Z - g\mu_B N H S$. c_n^\dagger and c_n are the spin-flip creation and annihilation operators at site n . Whenever the creation operator is applied to the ground-state, it leads to the excited state with the spin at site n flipped. In the present model, we will consider that the exchange coupling depends on the distance between nearest neighbor spins. We assume that, in the regime of small amplitude oscillations, this dependence is given by:

$$\begin{aligned} J_{n,n+1}^Z &\approx J_0 + \alpha(u_{n+1} - u_n), \\ J_{n,n+1}^{XY} &\approx J_0, \end{aligned} \quad (3)$$

where α is the effective spin-lattice coupling affecting the longitudinal spin-spin interactions. In what follows, an adiabatic approximation will be employed in order to solve the classical lattice motion equations. Within this approach, the time scale associated with the magnon dynamics is considered to be smaller than the time scale associated with the lattice vibrations.

Although this regime is usually not reached in ferromagnetic insulators, the recent advent of advanced materials exhibiting high-frequency terahertz magnons has impelled the development of a new class of ultrafast spintronic devices. Terahertz magnons have been reported, for example, in the 2D Ising honeycomb ferromagnet CrI_3 [33],

ultrathin film of ironpalladium alloys [34], layered iron-cobalt magnonic crystals [35] and noncollinear magnetic bilayers [36]. In this class of systems presenting high-frequency ferromagnetic magnons, the adiabatic integration over the phonon degrees of freedom can fairly incorporate the main influence of the underlying magnon-phonon coupling on the spin-wave dynamics.

Therefore we can consider $\dot{u}_n \approx 0$ and $\ddot{u}_n \approx 0$. It results in a direct relation between the lattice deformations and the magnon wave-function. Using this formalism, one can write an effective nonlinear Schrödinger equation for the magnon dynamics as:

$$\begin{aligned} i\hbar \dot{a}_n &= -\hbar^2 J_0 a_{n+1} - \hbar^2 J_0 a_{n-1} \\ &- \hbar^2 J_0 \chi (2|a_n|^2 + |a_{n+1}|^2 + |a_{n-1}|^2) a_n, \end{aligned} \quad (4)$$

from which a linear diagonal term has been omitted because it does not have any impact on the magnon dynamics. $|a_n|^2 = a_n^* a_n$ represents the probability of finding a spin deviation at site n . Moreover, the quantity $\chi = \alpha^2 \hbar^2 / \kappa J_0$ is a nonlinear parameter that measures the strength of the magnon-lattice coupling. In general lines, this equation represents a *modified discrete nonlinear Schrödinger equation (MDNLSE)* associated with the magnon dynamics.

Nonlinear contributions to the magnon dynamics also arise from magnon-magnon interactions and shown to induce the formation of magnetic solitons [37]. Recently, the competition between the nonlinear contribution resulting from a local anisotropy and disorder associated to a random magnetic field was investigated [38]. It has been demonstrated that large nonlinearities lead to the self-trapping of magnetic excitations which is anticipated by a sub-diffusive phase. Although self-trapping was shown to take place when the nonlinearity strength is much larger than the spectrum bandwidth, no precise bound between the sub-diffusion and the self-trapping phases was established. It is important to stress that while a local anisotropy leads to a nonlinear correction that depends only of the local magnon probability density [38], the present nonlinearity resulting from the magnon-phonon coupling also brings contributions from the magnon density at the neighboring sites. A generalization of the nonlinear term to account for a variable relative contribution of local and neighboring densities would simultaneously incorporate effects from both magnon-magnon and magnon-phonon interactions.

We will solve numerically Eq. (4) to follow the time-evolution of spin excitations. For the initial condition, we will use a single spin flip at the chain center ($n = 0$ will be taken as the center of chain). We will consider $t_m = 1/(\hbar J_0)$ as the relevant time unit. To analyze the main features of the spin-wave dynamics, we will compute the return probability defined as:

$$R_0 = |a_0|^2 \quad (5)$$

and the participation number defined as:

$$\xi = \frac{\sum |a_n|^2}{\sum |a_n|^4} \quad (6)$$

R_0 and ξ are two relevant quantities that can probe both the localization and self-trapping phenomena. If $R_0 > 0$ after a long-time run, a fraction of the initial spin excitations remains trapped around its initial location. ξ is an estimation of the number of sites over which the wave-packet is predominantly distributed. ξ remaining finite in the long-time regime signals the formation of stable localized wave-packets.

We will also compute the Shannon entropy associated to the evolving wave-packet defined as

$$S = - \sum_n |a_n|^2 \ln |a_n|^2, \quad (7)$$

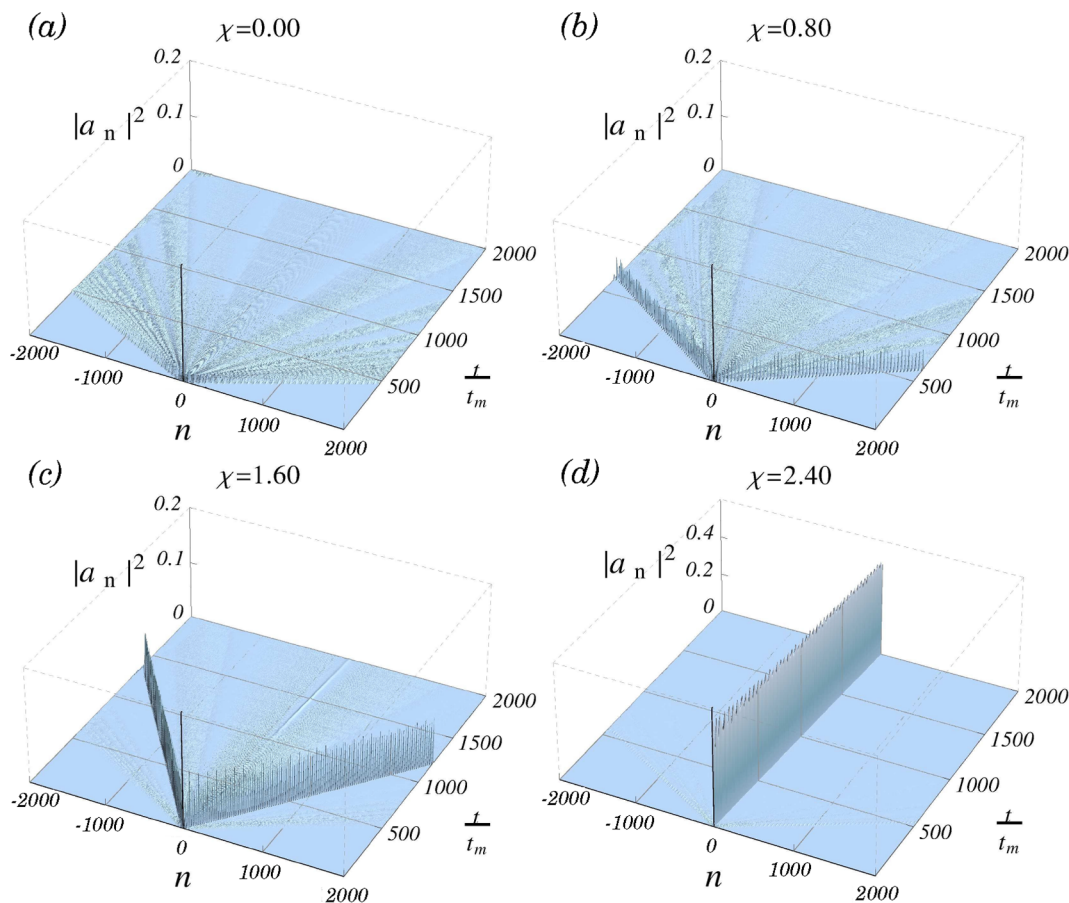


Fig. 2. Time evolution of the wave-function profile ($|a_n(t)|^2$) on a chain with sites indexed by n for (a) $\chi = 0.0$, (b) $\chi = 0.80$, (c) $\chi = 1.60$, (d) $\chi = 2.40$. While in absence of nonlinearity the wave function spreads over the lattice (see fig.a), the emergence of a soliton-like propagating structure characterizes the intermediate regime (see fig.b-c). Self-trapping is observed for strong nonlinearities (see fig.d).

which can give additional information regarding the wave-packet dynamics.

3. Results

We solved the set of discrete nonlinear Schrödinger equations using a standard Runge-Kutta algorithm. The numerical integration was performed considering a self-expanding algorithm of the chain size in order to avoid finite-size and border effects. The position $n = 0$ was taken as the chain center. All calculations were done by considering the initial condition $a_n(t = 0) = \delta_{n,0}$.

In Fig. 2 we plot the wave-function profile ($|a_n(t)|^2$) versus time t and spin position n for some representative values of the nonlinear parameter χ . In the linear case ($\chi = 0$) the initially localized spin excitation radiates over the chain evolving to a fully delocalized state. For large nonlinearities, a finite fraction of the spin excitation remains trapped around its initial location. For weak nonlinearities, breathing propagating soliton-like modes are developed, while a fraction of the magnon wave radiates. The velocity of the propagating solitons decreases as the nonlinearity is increased. In Fig. 3 we illustrate the transition between these two regimes. For $\chi = 1.82$, as shown in Fig. 3a, the moving breathing soliton has a very small velocity. Slightly above this point (see. eg. Fig. 3b), it remains trapped.

To precisely locate the self-trapping transition point, we will explore the behavior of the soliton velocity as a function of the nonlinear strength. At first, we followed the time-evolution of the position of the

wave-function maxima for several values of χ , as shown in Fig. 4a. Both maxima at the left and right branches are reported. They have the same velocity as expected due to the parity symmetry of the Hamiltonian and of the initial wave-function. This figure shows that the soliton velocity continuously decreases, vanishing above some characteristic nonlinearity. This feature is more clearly reported in Fig. 4b where the estimated values of the soliton velocity are plotted as a function of χ . We also performed a scaling analysis of the soliton velocity to provide an accurate estimate of the critical nonlinearity. In the vicinity of the critical point, the velocity shall decrease as a power-law $v \propto (\chi_c - \chi)^\beta$. The best power-law fit is achieved for $\chi_c = 1.825$ providing the decay exponent $\beta = 1/2$ (see Fig. 4c). This value is of the same order of magnitude of the critical nonlinearity for the transition from sub-diffusion to self-trapping of magnetic excitations that takes place in the presence of a random magnetic field acting together with a local anisotropy [38]. In such system, nonlinearity effectively accounts for the magnon-magnon interaction promoted by the local anisotropy. The present result gives further support to the general picture that self-trapping occurs when the nonlinearity strength sufficiently exceeds the spectrum bandwidth.

The return probability can also be used to signal the self-trapping transition. In Fig. 5 we report the return probability after a long time run as a function of χ . It is vanishing small below the critical point and becomes finite above χ_c . However, in contrast to the continuous vanishing of the soliton velocity, the return probability is discontinuous at the transition, with a jump $\Delta R_0(\chi_c) \approx 0.16$. The emergence of a

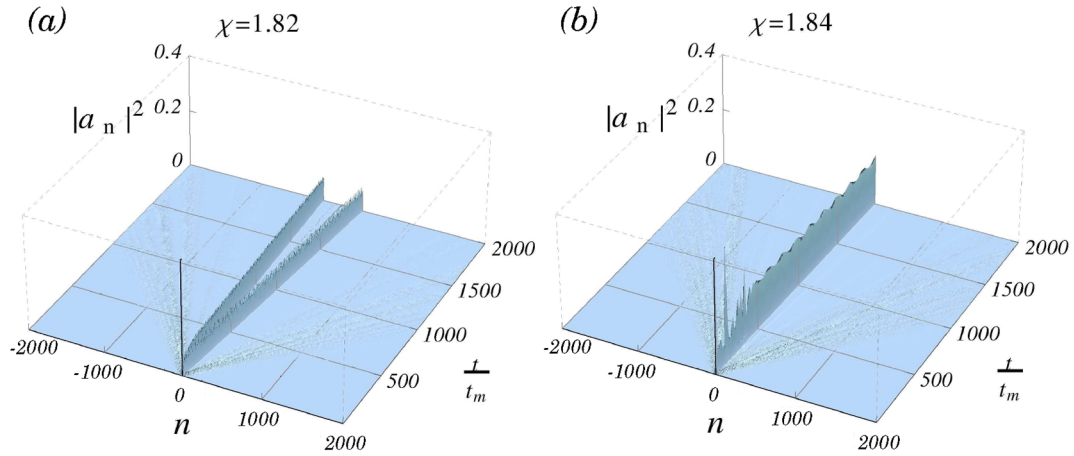


Fig. 3. Time evolution of the wave-function profile ($|a_n(t)|^2$) on the lattice sites n for (a) $\chi = 1.82$ and (b) $\chi = 1.84$. Notice the transition between the regimes of slowly propagating solitonic modes to self-trapping.

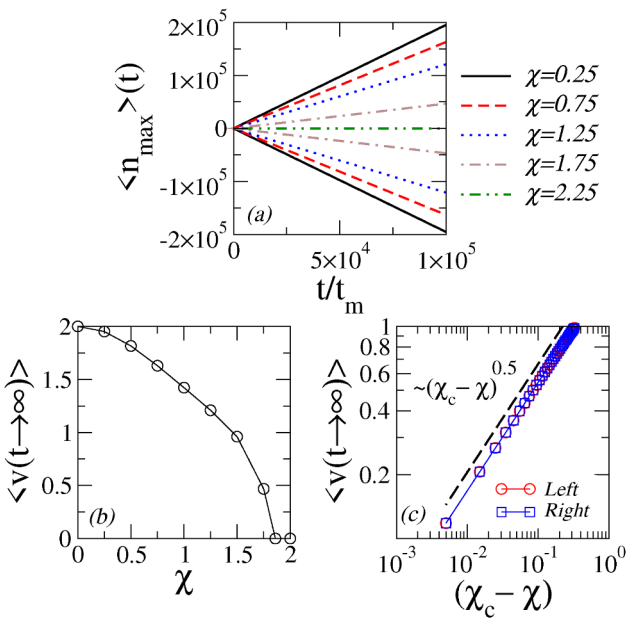


Fig. 4. Dynamics of soliton-like structures, with (a) the position of the solitonic waves ($\langle n_{max} \rangle(t)$) versus t for several values of χ , (b) the soliton velocity versus χ and (c) the scaling analysis of the velocity of both travelling solitons. The best fit to a power-law decay provides $\chi_c = 1.825$ and $v \propto (\chi_c - \chi)^{1/2}$.

discontinuous jump in the return probability is a direct consequence of the soliton trapping phenomenon. In the inset of Fig. 5, we plot the wave-function probability at the peak position of one of the travelling solitons slightly below χ_c . At the transition, both left and right solitons are trapped in the initial position, giving rise to a return probability which is twice as larger as the peak probability of each individual merging soliton.

The self-trapping transition leads to a distinct singularity in the wave-function spatial extension. In Fig. 6 the participation number dependence on the nonlinearity parameter χ is shown. It displays an overall $1/\chi^3$ decay, thus confirming the expected trend of strong localization promoted by nonlinearity. At the self-trapping critical point, the participation number develops a kink singularity. The merging of the two solitonic branches at χ_c does not result in a discontinuity of the

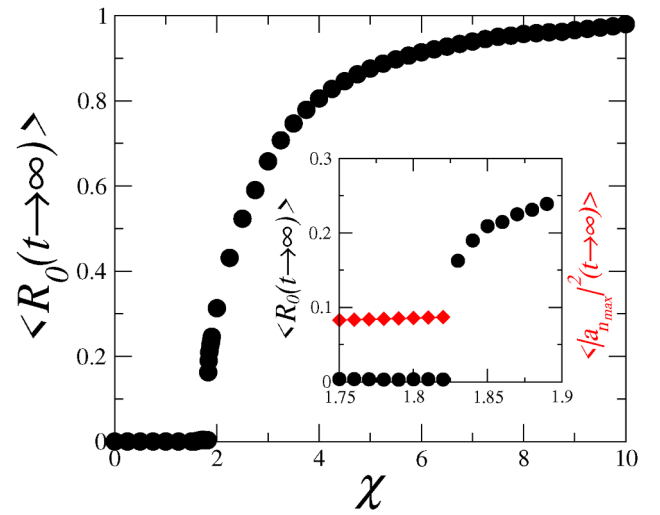


Fig. 5. Data of the long-time behavior of the return probability ($\langle R_0(t \rightarrow \infty) \rangle$) versus χ corroborates the transition for self-trapped waves at $\chi_c = 1.825$. The inset describes the χ -dependence of both return probability R_0 and the wave function probability at the center of the travelling soliton-like structures $|a_{max}|^2$. The merging of the two travelling solitons at χ_c leads to a discontinuous jump in R_0 .

participation number itself but in the rate it varies with χ .

The time-evolution of the Shannon entropy associated to the evolving wave-packet also signals the distinct dynamical regimes. To illustrate this aspect, we plot in Fig. 7a the time-dependence of the entropy for distinct values of the nonlinearity strength. It clearly depicts two scaling regimes. At short-times its logarithmic growth is fairly independent of χ for weak nonlinearities. This regime is associated with the initial spreading of the wave-packet and is suppressed for strong nonlinearities. After this transient regime, the entropy develops a slower increase. This feature results from the formation of the solitonic wave with a breathing pattern. In this regime, only the radiative component of the wave-packet contributes to the entropy overall increase. The slope of the $S \times \ln t$ curve can be used as an estimate of the wave-packet fraction carried by the radiating wave. It decreases exponentially with χ when the nonlinearity strength is enlarged, showing also a jump singularity at χ_c , as shown in Fig. 7b. This singularity is directly related to the merging of the solitonic branches at the self-

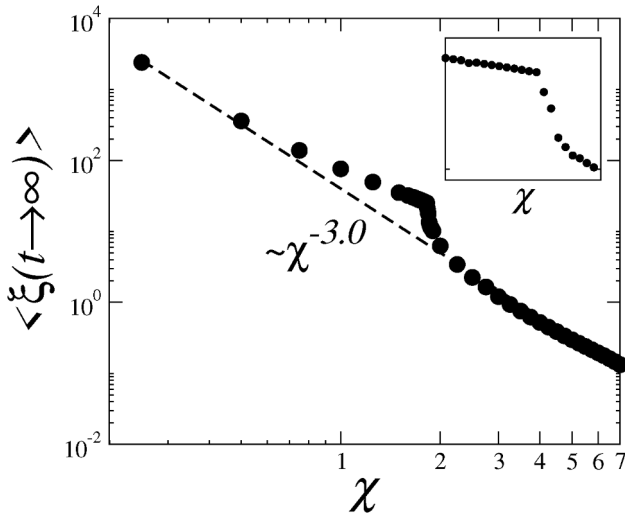


Fig. 6. Data of the long-time participation number ($\langle \xi(t \rightarrow \infty) \rangle$) versus χ . A kink singularity is developed at χ_c . The overall $1/\chi^3$ decay signals the strong localization promoted by nonlinearity.

trapping transition.

Before finishing, we would like to stress that the localized fraction of the wave-function, both above and below the self-trapping transition, has indeed a solitonic profile. In Fig. 8 we plot the spatial profiles of these localized structures for two representative values of the nonlinearity. For $\chi = 0.5$, we focus on one of the travelling soliton-like structures while for $\chi = 2$ we show a trapped mode localized around the initial position ($n = 0$). Both modes follow the well known soliton-like spatial profile proposed in Refs. [28,29] i.e., $|a_n(t)|^2 = |a_{n_{max}}|^2(t) \cdot \text{sech}^2[\gamma |a_{n_{max}}|^2(t)(n \pm vt)]$. The solid lines in Figs. 8 represent fittings using this profile, thus confirming the solitonic nature of these localized modes.

4. Summary

In this work we investigated the influence of lattice oscillations in the dynamics of initially localized one-magnon excitations in an anisotropic Heisenberg ferromagnetic chain. The magnon-lattice coupling was introduced by considering the longitudinal spin-spin exchange coupling as a linear function of the relative displacement between nearest-neighbor spins. Treating the lattice oscillations within a classical mechanics formalism and using an adiabatic approximation, the spin-wave dynamics is effectively described by a modified discrete nonlinear Schrödinger equation where the nonlinear parameter χ is proportional to the underlying spin-lattice coupling.

We showed that the nonlinearity promotes the wave-packet localization with the participation number presenting an overall $1/\chi^3$ decay. For weak nonlinearities, the wave-packet depicts both radiating and localized modes. The localized modes are left and right travelling breathing solitons. The soliton velocity decreases with χ , vanishing at $\chi_c = 1.825$. Above this point, the localized mode becomes self-trapped around the position of the initial excitation. We showed that the soliton velocity decays continuously as $(\chi_c - \chi)^{1/2}$. On the other hand, the return probability and participation number develop jump and kink singularities, respectively. The Shannon entropy was also shown to signal these distinct dynamical regimes. The present numerical results provide accurate estimates of the critical point and respective singularities of the relevant quantities associated with the presently reported nonlinear-induced self-trapping transition. It would be interesting to have these results derived from an analytical framework. It would bring valuable new insights to the overall wave dynamics in discrete nonlinear lattices.

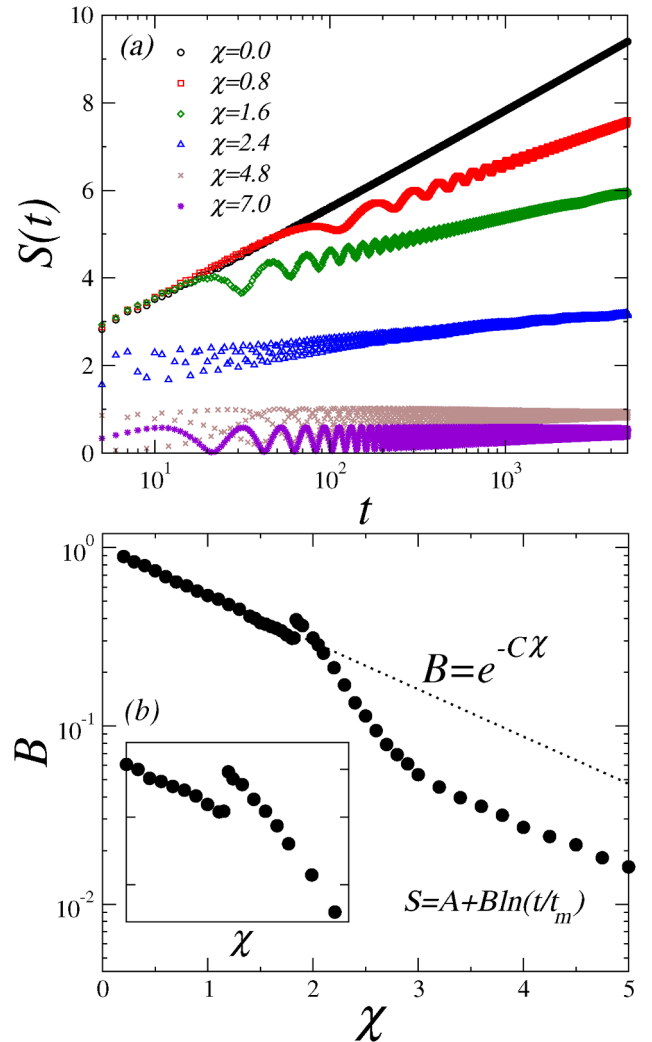


Fig. 7. (a) Time evolution of the Shannon entropy S for distinct values of the nonlinearity strengths χ . The logarithmic growth captures the wave-packet spreading. Notice that the slope changes at a characteristic time scale associated to the soliton formation. (b) The asymptotic slope of the entropy curves (in logarithmic time scale) as a function of the nonlinear strength. It gives an estimate of the radiative wave-packet fraction. The asymptotic slope changes discontinuously at the self-trapping transition.

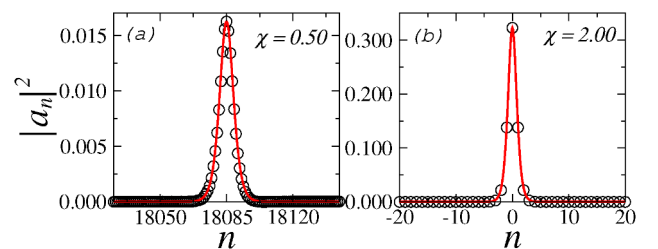


Fig. 8. The spatial profile of the wave-function around (a) travelling and (b) trapped solitonic modes. The solid lines represent a fitting curve, which corroborates a spatial profile $|a_n(t)|^2 = |a_{n_{max}}|^2(t) \cdot \text{sech}^2[\gamma |a_{n_{max}}|^2(t)(n \pm vt)]$ of breathing bright solitons.

CRediT authorship contribution statement

D. Morais: Conceptualization, Data curation, Investigation. **M.L. Lyra:** Writing - original draft, Supervision. **F.A.B.F. de Moura:** Validation, Writing - original draft. **W.S. Dias:** Methodology, Writing - review & editing, Data curation, Supervision.

Declaration of Competing Interest

The authors declare that they have no known competing financial interests or personal relationships that could have appeared to influence the work reported in this paper.

Acknowledgments

This work was partially supported by CNPq, CAPES, and FINEP (Federal Brazilian Agencies), and FAPEAL (Alagoas State Agency).

Appendix A. Supplementary data

Supplementary data associated with this article can be found, in the online version, at <https://doi.org/10.1016/j.jmmm.2020.166798>.

References

- [1] E. Pytte, Spin-phonon interactions in a heisenberg ferromagnet, *Ann. Phys.* 32 (3) (1965) 377–403, [https://doi.org/10.1016/0003-4916\(65\)90139-9](https://doi.org/10.1016/0003-4916(65)90139-9) URL: <http://www.sciencedirect.com/science/article/pii/0003491665901399>.
- [2] C.F. Kooi, Interaction of phonons and spin waves, *Phys. Rev.* 131 (1963) 1070–1075, <https://doi.org/10.1103/PhysRev.131.1070>.
- [3] R. Pradip, P. Piekarz, A. Bosak, D.G. Merkel, O. Waller, A. Seiler, A.I. Chumakov, R. Rüffer, A.M. Ole, K. Parlinski, M. Krisch, T. Baumbach, S. Stankov, Lattice dynamics of EUO: evidence for giant spin-phonon coupling, *Phys. Rev. Lett.* 116 (2016) 185501, <https://doi.org/10.1103/PhysRevLett.116.185501>.
- [4] P. Dai, H.Y. Hwang, J. Zhang, J.A. Fernandez-Baca, S.-W. Cheong, C. Kloc, Y. Tomioka, Y. Tokura, Magnon damping by magnon-phonon coupling in manganese perovskites, *Phys. Rev. B* 61 (2000) 9553–9557, <https://doi.org/10.1103/PhysRevB.61.9553>.
- [5] P. Reutler, F. Moussa, M. Hennion, F. Wang, A. Revcolevschi, Spin wave anomalies and phonons at low temperature in $\text{LaO}_{0.875}\text{Sr}_{0.125}\text{MnO}_3$, *J. Magn. Magn. Mater.* 242–245 (2002) 689–691, [https://doi.org/10.1016/S0304-8853\(01\)01022-8](https://doi.org/10.1016/S0304-8853(01)01022-8) proceedings of the Joint European Magnetic Symposia (JEMS'01). URL: <http://www.sciencedirect.com/science/article/pii/S0304885301010228>.
- [6] H. Man, Z. Shi, G. Xu, Y. Xu, X. Chen, S. Sullivan, J. Zhou, K. Xia, J. Shi, P. Dai, Direct observation of magnon-phonon coupling in yttrium iron garnet, *Phys. Rev. B* 96 (2017) 100406, <https://doi.org/10.1103/PhysRevB.96.100406>.
- [7] X. Li, D. Labanowski, S. Salahuddin, C.S. Lynch, Spin wave generation by surface acoustic waves, *J. Appl. Phys.* 122 (4) (2017) 043904, <https://doi.org/10.1063/1.4996102>.
- [8] A. Milosavljević, A. Olaj, J. Pei, Y. Liu, C. Petrovic, N. Lazarević, Z.V. Popović, Evidence of spin-phonon coupling in CrS_2 , *Phys. Rev. B* 98 (2018) 104306, <https://doi.org/10.1103/PhysRevB.98.104306>.
- [9] P.C. Lou, L. de Sousa Oliveira, C. Tang, A. Greaney, S. Kumar, Spin phonon interactions and magneto-thermal transport behavior in p-si, *Solid State Commun.* 238 (2018) 37–42, <https://doi.org/10.1016/j.ssc.2018.08.008> URL: <http://www.sciencedirect.com/science/article/pii/S0038109818304526>.
- [10] J. Holanda, D.S. Maior, A. Azevedo, S.M. Rezende, Detecting the phonon spin in magnon-phonon conversion experiments, *Nat. Phys.* 14 (5) (2018) 500–506, <https://doi.org/10.1038/s41567-018-0079-y>.
- [11] W. Heisenberg, Mehrkörperproblem und resonanz in der quantenmechanik, *Zeitschrift für Physik* 38 (6) (1926) 411–426, <https://doi.org/10.1007/BF01397160>.
- [12] W. Heisenberg, Zur theorie des ferromagnetismus, *Zeitschrift für Physik* 49 (9) (1928) 619–636, <https://doi.org/10.1007/BF01328601>.
- [13] V.L. Libero, K. Capelle, Spin-distribution functionals and correlation energy of the heisenberg model, *Phys. Rev. B* 68 (2003) 024423, <https://doi.org/10.1103/PhysRevB.68.024423>.
- [14] M. Belhadi, S. Kheffache, Magnons heat transport at an integrated nanostructure in ultrathin heisenberg ferromagnetic films, *Surf. Rev. Lett. (SRL)* 18 (06) (2011) 241–248, <https://doi.org/10.1142/S0218625X1101459X> URL: <https://ideas.repec.org/a/wsi/srlxxx/v18y2011i06ns0218625x1101459x.html>.
- [15] H. Wijesinha, K.A.I.L. Wijewardena Gamalath, Spin waves in two and three dimensional magnetic materials, *Int. Lett. Chem., Phys. Astron.* 49 (2015) 35–47, <https://doi.org/10.18052/www.scipress.com/IJLCPA.49.35>.
- [16] D.C. Mattis, *The Theory of Magnetism I: Statics and Dynamics*, Springer-Verlag, New York, 1981.
- [17] L. Liao, Y. Chen, Spin-wave theory applied to the low-temperature properties of the spin-1/2 ferromagnetic chain with the y-direction exchange anisotropy, *Superlattices Microstruct.* 73 (2014) 82–97, <https://doi.org/10.1016/j.spmi.2014.05.016> URL: <http://www.sciencedirect.com/science/article/pii/S074960361400161X>.
- [18] N. Laflorencie, D.J. Luitz, F. Alet, Spin-wave approach for entanglement entropies of the J₁-J₂ heisenberg antiferromagnet on the square lattice, *Phys. Rev. B* 92 (2015) 115126, <https://doi.org/10.1103/PhysRevB.92.115126>.
- [19] D. Maiti, D. Dey, M. Kumar, Frustrated spin-1/2 ladder with ferro- and antiferromagnetic legs, *J. Magn. Magn. Mater.* 446 (2018) 170–176, <https://doi.org/10.1016/j.jmmm.2017.09.025> URL: <http://www.sciencedirect.com/science/article/pii/S0304885317311964>.
- [20] P.A. Deymier, J.O. Vasseur, K. Runge, A. Manchon, O. Bou-Matar, Phonon-magnon resonant processes with relevance to acoustic spin pumping, *Phys. Rev. B* 90 (2014) 224421, <https://doi.org/10.1103/PhysRevB.90.224421>.
- [21] M. Mochizuki, N. Furukawa, N. Nagaosa, Theory of spin-phonon coupling in multiferroic manganese perovskites Rmno_3 , *Phys. Rev. B* 84 (2011) 144409, <https://doi.org/10.1103/PhysRevB.84.144409>.
- [22] M.E. Gouvêa, A.S.T. Pires, Effect of spin-phonon coupling on the haldane gap in antiferromagnetic heisenberg chains, *Phys. Rev. B* 75 (2007) 052401, <https://doi.org/10.1103/PhysRevB.75.052401>.
- [23] S.C. Guerreiro, S.M. Rezende, Magnon-phonon interconversion in a dynamically reconfigurable magnetic material, *Phys. Rev. B* 92 (2015) 214437, <https://doi.org/10.1103/PhysRevB.92.214437>.
- [24] M. Malard, A.S.T. Pires, Influence of magnon-phonon coupling on the phonon dynamics of one-dimensional antiferromagnets, *Phys. Rev. B* 76 (2007) 104407, <https://doi.org/10.1103/PhysRevB.76.104407>.
- [25] Y. Huang, L. Pi, Y. Zhang, Effects of spin-phonon interaction on transport, magnetic properties and the oxygen isotope effect in r1-xaxmno_3 , *J. Magn. Magn. Mater.* 323 (22) (2011) 2764–2769, <https://doi.org/10.1016/j.jmmm.2011.05.043> URL: <http://www.sciencedirect.com/science/article/pii/S030488531100312X>.
- [26] J. Zhao, D.T. Adroja, D.-X. Yao, R. Bewley, S. Li, X.F. Wang, G. Wu, X.H. Chen, J. Hu, P. Dai, Spin waves and magnetic exchange interactions in CaFe_2As_2 , *Nat. Phys.* 5 (8) (2009) 555–560, <https://doi.org/10.1038/nphys1336>.
- [27] K. Shen, G.E.W. Bauer, Laser-induced spatiotemporal dynamics of magnetic films, *Phys. Rev. Lett.* 115 (2015) 197201, <https://doi.org/10.1103/PhysRevLett.115.197201>.
- [28] T. Holstein, Studies of polaron motion: Part i. the molecular-crystal model, *Ann. Phys.* 8 (3) (1959) 325–342, [https://doi.org/10.1016/0003-4916\(59\)90002-8](https://doi.org/10.1016/0003-4916(59)90002-8) URL: <http://www.sciencedirect.com/science/article/pii/0003491659900028>.
- [29] T. Holstein, Studies of polaron motion: Part ii. the "small" polaron, *Ann. Phys.* 8 (3) (1959) 343–389, [https://doi.org/10.1016/0003-4916\(59\)90003-X](https://doi.org/10.1016/0003-4916(59)90003-X) URL: <http://www.sciencedirect.com/science/article/pii/000349165990003X>.
- [30] W.P. Su, J.R. Schrieffer, A.J. Heeger, Solitons in polyacetylene, *Phys. Rev. Lett.* 42 (1979) 1698–1701, <https://doi.org/10.1103/PhysRevLett.42.1698>.
- [31] W.P. Su, J.R. Schrieffer, A.J. Heeger, Soliton excitations in polyacetylene, *Phys. Rev. B* 22 (1980) 2099–2111, <https://doi.org/10.1103/PhysRevB.22.2099>.
- [32] A.S. Davydov, N.I. Kislukha, Solitons in one-dimensional molecular chains, *Phys. Status Solidi (b)* 75 (2) (1976) 735–742, <https://doi.org/10.1002/psb.2220750238> URL: <https://onlinelibrary.wiley.com/doi/abs/10.1002/psb.2220750238>.
- [33] W. Jin, H.H. Kim, Z. Ye, S. Li, P. Rezaie, F. Diaz, S. Siddiq, E. Wauer, B. Yang, C. Li, S. Tian, K. Sun, H. Lei, A.W. Tsen, L. Zhao, R. He, Raman fingerprint of two-ahertz spin wave branches in a two-dimensional honeycomb insulating ferromagnet, *Nat. Commun.* 9 (2018) 5122, <https://doi.org/10.1038/s41467-018-07547-6>.
- [34] H.J. Qin, K. Zakeri, A. Ernst, L.M. Sandratskii, P. Buczek, A. Marmodoro, T.H. Chuang, Y. Zhang, J. Kirschner, Long-living terahertz magnons in ultrathin metallic ferromagnets, *Nat. Commun.* 6 (2015) 6126, <https://doi.org/10.1038/ncomms7126>.
- [35] H.J. Qin, S. Tsurkan, A. Ernst, K. Zakeri, Experimental realization of atomic-scale magnonic crystals, *Phys. Rev. Lett.* 123 (2019) 257202, <https://doi.org/10.1103/PhysRevLett.123.257202>.
- [36] M.L.M. Laliou, R. Lavrijsen, R.A. Duine, B. Koopmans, Investigating optically excited terahertz standing spin waves using noncollinear magnetic bilayers, *Phys. Rev. B* 99 (2019) 184439, <https://doi.org/10.1103/PhysRevB.99.184439>.
- [37] A. Kosevich, B. Ivanov, A. Kovalev, Magnetic solitons, *Phys. Rep.* 194 (3) (1990) 117–238, [https://doi.org/10.1016/0370-1573\(90\)90130-T](https://doi.org/10.1016/0370-1573(90)90130-T) URL: <http://www.sciencedirect.com/science/article/pii/037015739090130T>.
- [38] C. Wang, Y. Cao, X.R. Wang, P. Yan, Interplay of wave localization and turbulence in spin seebeck effect, *Phys. Rev. B* 98 (2018) 144417, <https://doi.org/10.1103/PhysRevB.98.144417>.